Climate-related variations in mixing dynamics in an Alaskan arctic lake

Sally MacIntyre,[a,b*] Jonathan P. Fram,[b] Paul J. Kushner,[c] Neil D. Bettez,[d] W. J. O'Brien,[e] J. E. Hobbie,[f] and George W. Kling[g]

[a]Department of Ecology, Evolution and Marine Biology, University of California, Santa Barbara, California

[b]Marine Science Institute, University of California, Santa Barbara, California

[c]Department of Physics, University of Toronto, Toronto, Ontario, Canada

[d]Department of Ecology and Evolutionary Biology, Cornell University, Ithaca, New York

[e]Department of Biology, University of North Carolina at Greensboro, Greensboro, North Carolina

[f]The Ecosystems Center, Marine Biological Laboratory, Woods Hole, Massachusetts

[g]Department of Ecology and Evolution, University of Michigan, Ann Arbor, Michigan

Running head: Mixing dynamics in an arctic lake

*Corresponding author: (sally@icess.ucsb.edu)

Acknowledgements

We thank Jim Laundre, James King, Chris Wallace, Chris Crockett, Christie Haupert, Mary Anne Evans, Lorenz Moosmann, Arron Layns, Bridget Benson, Rebecca Lawson, Karen Jo Riseng, Amanda Fields, Robyn Smyth, Avrey Parsons-Field, Jeremy Meirs, Dan White, Cody Johnson, and Sandy Roll for help with field measurements, and Brice Loose, Lorenz Moosmann, Chad Helmle, Chris Wallace, and Arron Layns for assistance with processing and analysis of physical data. The contributions of two anonymous reviewers are gratefully acknowledged. The Arctic Long Term Ecological Research (LTER) Project provided meteorological and hydrographic data. Financial support was provided by National Science Foundation Division of Environmental Biology (DEB)-0508570, -0423385, -9810222, Office of Polar Programs (OPP)-9911278 to the Arctic LTER and DEB-9726932, -0108572, -0640953, Ocean Sciences (OCE)-9906924, and Arctic Natural Sciences (ARC)-0714085 to SM.

Abstract

Mean epilimnetic temperatures from mid-June through mid-August in a small, arctic kettle lake had no trend from 1975 to 2008 and varied annually up to $\pm 3^{o}C$ relative to the mean. Analysis of data from temperature arrays deployed on the lake from 1998-2007 showed that as mean summer temperatures shifted from $2.5^{o}C$ below the mean, to the mean, and $3^{o}C$ above the mean, deepening of the mixed layer during cold fronts decreased, average metalimnetic thickness increased from 2 to 5 m, maximum values of water-column stability increased fourfold, minimum values of Lake numbers (L_N) increased from ≤ 1 to 10, the metalimnetic coefficient of eddy diffusivity (K_z) decreased from 10^{-5} m^2 s^{-1} to 10^{-7} m^2 s^{-1}, and time scales for mixing across the metalimnion increased from days to months. Mean surface temperatures and mixing regimes were not significantly correlated with mean air temperatures, mean insolation, or mean wind speeds during summer, but instead depended upon the frequency and persistence of events with higher winds, heating, or cooling. In summers with cold surface temperatures, the surface energy fluxes which induce mixing by heat loss were low, but with frequent wind events, heat was mixed downwards leading to lower stability. The warmest surface temperatures resulted when atmospheric conditions led to persistent positive buoyancy flux in early summer and winds were elevated primarily on diel cycles as opposed to longer ones. Summers with cooler water temperatures and enhanced vertical mixing are linked to frontal activity and low atmospheric pressure near the Alaskan coast.

The mixing dynamics of lakes during the stratified period depend upon the heating, cooling, and wind forcing at a lake's surface. Our understanding of mixing dynamics, however, has been developed based on process studies of a few days to a few weeks duration. For instance, Imberger (1985) quantified the role of evaporation, sensible heat exchange, net radiation, and wind driven shear at the base of the mixed layer in forming and deepening the diurnal mixed layer in a subtropical reservoir, and MacIntyre et al. (2002) illustrated the importance of evaporation in driving mixed layer deepening in a shallow tropical lake. Mixing within the metalimnion and hypolimnion is mediated by internal waves (Saggio and Imberger 1998), and a combination of laboratory and field studies have shown that two dimensionless indices, the Wedderburn (W) and Lake numbers (L_N), which are based on water column stability, wind shear, and basin dimension (Imberger and Patterson 1990), can be used to predict 1) the degree of tilting of the thermocline (Monismith 1986), 2) the type of internal waves generated (Horn et al. 2001; Boegman et al. 2005), and 3) incidence of turbulence in the meta and hypolimnion (MacIntyre et al. 1999; MacIntyre et al. 2006).

A few longer term studies have characterized the frequency of mixing events in response to variable surface forcing and their consequences for thermal structure (Talling 1966; Lewis 1973; Yeates and Imberger 2004). Further development of our quantitative understanding of which processes drive mixing at different latitudes and for lakes of different sizes requires budgets describing the magnitude and variation in surface forcing, estimates of the frequency and intensity of mixing events and the changing efficacy of various mixing processes during the stratified period, and knowledge of how climate affects surface forcing on seasonal or interannual time scales.

Quantifying patterns in stratification and variance in mixing dynamics in lakes requires consideration of the spatial and temporal scales involved in surface forcing. Classically, regional climate is set by latitude and by local geographical factors such as proximity to coasts and topography. These factors determine average insolation, humidity, wind patterns, and precipitation (Kalff 2001). The wind-driven and thermally-driven surface forcing that causes mixing depends nonlinearly on the meteorological fields. Thus, the average meteorology does not determine average lake mixing (see Monahan 2006 for a related discussion in the context of oceanic wind stress variability). Instead, the surface forcing is determined by the spectrum of atmospheric variability on daily, synoptic, and longer timescales. The controls on lake physics imposed by this meteorological variability are both temporally and spatially 'non-local'. For example, spatial patterns of atmospheric variability correlate local meteorology with continental-scale and even planetary-scale circulation patterns such as the Arctic Oscillation and the Pacific Decadal Oscillation. These and other large-scale patterns control local winds, temperature extremes, and synoptic variability as expressed through the frequency of transitions between warm and cold fronts (Thompson and Wallace 2001; Overland et al. 2004; Serreze and Barrett 2008). The large-scale patterns correlate well with parameters relevant to stratification in lakes, such as ice on - off dates in boreal and Arctic lakes (Bonsal et al. 2006), but their relation to mixing dynamics has not yet been examined.

The mixing dynamics of arctic lakes deep enough to stratify and whose surface temperatures exceed 4^{o}C after ice off are relatively unexplored (Vincent et al. 2008). Data obtained for one ice free season in a small arctic lake indicated that L_N varies from less than 1 to over 100, that increases in vertical mixing occur when $L_N \approx 1$, and that the lowest values

of L_N occurred during shifts between warm and cold fronts (MacIntyre et al. 2006). Thus, several mixing regimes occur within this one lake. For low L_N ($L_N \leq 1$), fluxes of solutes and particles from the lower to the upper water column can be brought about by instabilities in the internal wave field and by wind-driven upwelling and associated horizontal and vertical mixing. For intermediate L_N ($1 < L_N < 10$), mixing is caused primarily by instabilities in the internal wave field, and wind-driven upwelling no longer plays a role. For high L_N ($L_N > 10$) the internal wave mechanism is suppressed. For all these regimes, the mixed layer can deepen due to cooling, and the resulting entrainment can cause vertical fluxes. For the regime $L_N > 10$, mixed layer deepening is the only remaining turbulent process which causes vertical exchange.

Climate change could affect the proportion of time that L_N is low, intermediate, or high, and each regime has implications for vertical fluxes of solutes and particles. For example, if climate change leads to strong epilimnetic warming, increased stratification of the water column could shift minimum values of L_N from the low to the intermediate regime or from the intermediate to the high regime. The diminished mixing from such shifts might be partially offset by enhanced evaporative heat loss, but exchanges between the upper and lower water column may be reduced because mixed layer deepening is proportional to the flux of turbulent kinetic energy into a lake from heat loss and wind but inversely proportional to the temperature gradient across the metalimnion (Fisher et al. 1979). The magnitude of L_N and evaporation also depend strongly on wind forcing for which we lack clear forecasts under climate change. Whether the mixing dynamics of stratified, arctic lakes shift from regimes in which vertical fluxes are due to the combination of wind-induced movement of the thermocline and surface heat losses ($L_N < 10$) to ones in which they are primarily driven

by surface heat loss (L_N>10) will depend not only on air temperatures but also on factors which influence wind velocity.

Several lines of evidence suggest that factors influencing mixing dynamics in lakes in arctic Alaska are more complicated than would be predicted by increasing temperatures alone. At Barrow, AK, where the longest meteorological record is available from the Alaskan arctic, the temperature change from 1949-2005 was 1.9^{o}C with the largest changes in winter and spring (Shulski and Wendler 2007). The Pacific Decadal Oscillation strongly influenced the signal such that temperatures from 1949 to 1975 were colder than those from 1977 until 2005. Since 1976, annual temperatures at Barrow have increased slowly, but the increase has been most muted in summer. Similar patterns of larger temperature increases in winter and spring and smaller increases in summer have been found for the Arctic as a whole (Serreze et al. 2000). The number of cyclones (low pressure systems), with consequent shifts between warm and cold air masses, is dependent upon the phase of the Arctic Oscillation in summer and sets summer apart from winter in the Arctic (Serreze and Barrett 2008). During its positive phase, low pressure is centered over the North Pole, cyclogenesis is higher, air temperatures in northern Alaska are colder, and tropospheric winds flow from the north. During its negative phase, fewer cyclones are generated, high pressure dominates the Beaufort Sea, air temperatures in northern Alaska are warmer, and tropospheric winds are reduced. Thus, mixing patterns and dynamics in Alaskan arctic lakes will likely be influenced by global warming and by larger scale atmospheric patterns which modify frontal dynamics.

The goal of this paper is to quantify variations in mixing dynamics during the ice-free period in Toolik Lake, an arctic lake on the North Slope of Alaska, in the context of

changing atmospheric forcing. Toolik Lake is the site of long-term measurements by the Arctic Long Term Ecological Research (LTER) Project with surface water temperatures first available in 1975 and meteorological data first available in 1988. We extend the record of surface water temperatures from the ice-free season first presented by McDonald et al. (1996) and assess whether the warming trend continued. Beginning in 1998, we deployed a meteorological station on the lake as well as one or more temperature arrays within the lake. We compute surface energy budgets and contrast the frequency of events with high winds or cooling, the energy in the wind field, buoyancy flux, the stability of the lake, the flux of turbulent kinetic energy relative to stability, L_N, and K_z. With this analysis, we develop a mechanistic understanding of how the variability in surface forcing leads to short term and year to year variations in the lake's stability and to its sensitivity to mixing due to winds and cooling events. Our understanding of mixing dynamics is extended to the longer time series by relating mean lake stability and L_N to mean surface water temperatures, and is extended to future climate regimes by relating mixing to atmospheric cycles and potential changes in frontal activity.

Site description

Toolik Lake, Alaska (68°38'N, 149°38'W) , in the northern foothills of the Brooks Range, is an oligotrophic multi-basin kettle lake with a surface area of 1.5 km^2, mean depth of 7.1 m, and maximum depth of 25 m (Fig. 1). Ice off occurs near summer solstice when solar radiation is near maximal values, and stratification quickly follows (O'Brien et al. 1997). The topography around Toolik Lake is described by Miller et al. (1986) and consists of low rolling hills covered with small shrubs and tussock tundra. Thus, without fringing trees, the atmospheric boundary layer can rapidly adjust from land to water and the

momentum from the wind is transferred to the lake within a short distance from land. Southerly winds are common and result in warmer, boreal air masses rising over the Brooks Range and descending to Toolik. In 2004 these air masses brought tremendous amounts of smoke from fires on the south slope of the Brooks Range. Increased wind, cloudiness, and occasionally precipitation accompany the movement of cold fronts into the region. Attenuation of light is relatively high (diffuse attenuation coefficient, k_d, ~ 0.5 to 0.9 m^{-1}) due to high concentrations of chromophoric dissolved organic matter in the lake. Epilimnetic chlorophyll concentrations are low (0.5 – 2 μg L^{-1}) (Miller et al. 1986). The basic limnology of the lake is reviewed in O'Brien et al. (1997). MacIntyre et al. (2006) present physical pathways of nutrient supply in the ice free season.

Methods

Meteorological and radiation measurements - Data for this study were collected at two main sites. Beginning in 1988, data have been measured at a land-based meteorological station located within 50 m of the lake shore. Variables measured include hourly wind speed and direction at 1 and 5 m height, air temperature and relative humidity, photosynthetically available radiation, short wave radiation, and barometric pressure. Beginning in 1990, lake surface elevation and water temperature (Onset Stowaway with 0.2^{o}C accuracy and 3 minute time constant) at 2 m depth were recorded and stored as 3 hour averages. Instrumentation is described at: http://ecosystems.mbl.edu/arc/weather/tl/index.shtml. Beginning in 1998, five minute averaged wind speed and direction, relative humidity, air temperature, and upwelling and downwelling short wave and long wave radiation were obtained on a floating meteorological station anchored in the main basin of the lake (Fig. 1). The station was deployed as soon after ice off as possible. Instrumentation and sampling are described in

MacIntyre et al. (2006); water temperatures in the upper 5 cm were measured with a shielded self-contained temperature logger (0.002^{o}C accuracy, Oregon Environmental Instruments in 1998 and 1999, RBR TR1050 in subsequent years). Additional details on the meteorological data collected on the lake are found at: http://ecosystems.mbl.edu/arc/landwater/lake_climate/index.shtml. Gaps in the data due to instrument failures were filled using data from the land-based station using linear regressions at times when both systems were functioning. For greater accuracy in computing shear stress, a function was determined based on spectral analysis of the 5 minute averaged wind speed to convert the hourly wind data to 5 minute wind data. When gaps occurred in long wave data, data were obtained from nearby Imnavait Basin (N 68^{o} 36' 58.6", W 149^{o} 18' 13.0", 937 m ASL) and net long wave was computed using linear regression for times when both systems were functioning. Data collection failed on 20 July 2006, and regressed data from the land-based station, with the exception of long wave data, were used for the second half of the summer. No long wave data were collected from Imnavait in 2006, so data from the Kuparuk Basin (N 68^{o} 38' 24.5" W 149 ^{o} 24' 23.4" 774 m ASL) were used. A data gap from 5 Aug to 22 Aug at the Kuparuk was filled using linear regression including measured downwelling short wave radiation and downwelling clear sky radiation. In 1999-2004, the upper limit for incoming short wave radiation was set at 800 W m^{-2} and irradiance data on the lake were collected only once every 5 minutes. Subsequently, the upper bound for short wave was increased above 1000 W m^{-2} and 5 minute average data were collected. The diffuse attenuation coefficient was calculated using Beers Law from measurements of photosynthetic photon flux density measured weekly with an underwater quantum sensor (LI-COR LI-192SA sensor, LI-185 meter) at 0.5-m intervals.

Time-series measurements of temperature – Beginning in 1998, water column temperatures were measured at ten second intervals at two or more sites in the main basin (Fig. 1) for the ice free period using self-contained temperature loggers on taut-line moorings. These were installed within a week of ice off and deployed through mid-August. The subsurface float was located ~1 m below the air-water interface. To measure temperature in the upper water column, one logger was directly mounted below a Styrofoam float which shielded it from direct insolation. One to three loggers were typically suspended below the surface float from a weighted line. Standard moorings were located adjacent to the meteorological station at Toolik Main (TM, typically 20 to 25 depths) where bottom slopes are low and at Central (CN, typically 10 to 20 depths) where the thermocline comes into contact with the sloping bottom boundary. The temperature array in 2007 was retrieved on 10 August. To obtain a full record for this study, we combined the data set from the array at TM, an overwintering thermistor chain deployed at TM, and an additional array of 6 temperature loggers deployed adjacent to the overwintering chain on 11 August. The uppermost logger in this array was located 1 m below the surface. The depth of the actively mixing layer for this later period was estimated based on temperatures relative to those of this logger, and the depth of the shallowest actively mixing layer was assumed to be 1 m. Instrumentation used from 1998-1999 are described in MacIntyre et al. (2006); RBR TR1050 loggers, with accuracy of 0.002^{o}C and time constant of 3 seconds, were used since 2000 with data from occasional malfunctioning loggers supplemented with that from Onset Stowaways (accuracy 0.2^{o}C and time constant 3 minutes) in 2000.

Profile data - Conductivity, temperature, and depth (CTD) profiles were obtained from the surface to 16 to 18 m from 1975 to the present at ~ weekly intervals between ice off,

which occurs typically in the latter half of June, to mid-August with a Hydrolab water quality sonde. Accuracy of the temperature measurements is 0.1^{o}C. Temperature calibration was performed prior to the beginning of each field season.

Analysis of long term temperature data from Toolik Lake – Mean surface temperatures were computed from 19 June to 23 August of each year from CTD casts taken since 1975 and from the temperature logger located 2 m below the air-water interface since 1990. To enable comparison of these two approaches, we defined mean surface temperature as that at two meters and computed it from the CTD data by taking the mean of the measurements at 1 and 3 m when no measurements were available at 2 m. We additionally used the continuous data to check whether the surface temperatures from the CTD data were biased high due to sampling in the day or by avoiding inclement conditions. The only substantive discrepancy between the two approaches occurred in 1999 when the mean epilimnetic temperatures from the CTD casts were biased low due to two profiles in early summer when the lake temperatures were still cold (Fig. 2A). The lake subsequently warmed up and remained warm for the rest of the sampling period. We computed mean temperature and stability for the dates above using the CTD casts. Temperatures were available from 0 m, 1 m, 3 m, 5 m, 8 m, 12 m, and 16 m through 1990. Data were available every meter in subsequent years, but calculations were done only for the upper 16 m to be consistent with data collection in earlier years. CTD casts were not available in 1982, 1990, and 1993.

Time series computations with meteorological and temperature data in the lake – Sensible and latent heat exchanges, surface energy fluxes, depth of the upper mixing layer, buoyancy flux, effective heat flux into the upper mixing layer, air and water friction velocities u_* and u_{*w} (also known as the turbulent velocity scale from wind), turbulent

velocity due to heat loss w_*, and flux of turbulent kinetic energy into the mixed layer were calculated as in MacIntyre et al. (2002) following Imberger (1985). We present the meteorological and surface energy budget calculations as half hour averages. We calculated the coefficient of eddy diffusivity in the upper mixing layer as $K_z = c_1 q l$ where q is the turbulent velocity scale and l is the turbulent length scale (Tennekes and Lumley 1972), and we let c_1, which takes into account the inefficiency of mixing in the upper water column, be 0.7 (MacIntyre 1993). The turbulent velocity scale is computed from the turbulent velocity scales for heat loss and wind as $q = (w_*^3 + c_n^3 u_{*w3})^{1/3}$ where $c_n^3 = 1.23$ (Fisher et al. 1979). For turbulence near the surface, l is the depth of the active mixing layer defined as the uppermost layer in which temperatures are within 0.02°C of the surface temperature. This approach estimates K_z in the upper mixing layer when it was turbulent due to wind and heat loss.

Depths of isotherms, specific conductivity, salinity, density, and L_N were computed as in MacIntyre et al. (1999, 2006). We compute L_N rather than the Wedderburn number because we are interested in the dynamics of the seasonal thermocline and because of the difficulty in accurately specifying the top of the seasonal thermocline as needed to calculate W. The periods of first vertical mode internal waves (T_1) range from 9 hours during weakly stratified conditions near ice off to more typical summer values between 3 and 5 hours (Evans et al. 2008). L_N was temporally filtered over one ¼ T_1; we set T_1 at 4 hours. Stability was calculated following Idso (1973) and expressed as J m^{-2}. Mean lake temperature, stability, and L_N were computed using the bathymetry of the main basin of the lake. Two-day average values of K_z for the main basin were calculated using the heat budget method of Jassby and Powell (1975) with the 10-second thermistor string data Gaussian filtered for a

two day period to avoid contamination of the heat budgets by internal wave motions. The heat budget approach is valid when and where the lake is gaining heat and lateral advection is minor.

Results

Mean epilimnetic temperatures from mid-June through mid-August for the 33 years averaged ~ 11.6^{o}C. There was no trend to the data (Fig. 2A). The estimates of mean epilimnetic temperature were similar using the CTD casts and the time series temperature data from 2 m. This similarity validates the earlier observations taken with the CTD alone. The lack of a trend and high variance were also found when using just the surface values of temperature and when temperatures were obtained by linearly interpolating between the surface and 5 m to get a 0 – 5 m average value. A slight trend upward is evident if averaging is done for July alone (Hinzman et al. 2005), but then a negative trend is evident for the second half of summer (data not shown). For the 33 years, average mean temperatures tended to be 2^{o}C cooler or warmer than the mean except for two particularly cold years, 1981 and 2003 when mean surface temperatures were 9^{o}C, and four particularly warm years, 1987, 1988, 1998 and 2007 when mean surface temperatures were between 13.5^{o}C and 15^{o}C. Years in which air temperatures were warm were not necessarily years in which surface water temperatures were warm (Fig. 2B).

To develop a mechanistic understanding of the differences in stratification and mixing dynamics in summers when surface water temperatures were warm versus cold, and to understand how differences in surface forcing led to these dynamics, we compared conditions in 2003 when mean surface temperatures were 2.5^{o}C below the mean (Fig. 3A), in 2004 when surface temperatures were ~1^{o}C above the mean (2004, Fig. 4A), in 2006 when

water temperatures were near average (Fig. 5A), and in 2007 when surface water temperatures were more than 3^{o}C above the mean (Fig. 6A). In all years, two to three warming events occurred which increased stratification in the upper water column. In warm as opposed to cold years, the upper mixed layer was shallower, the temperature gradient at the top of metalimnion tended to be larger, the metalimnion was thicker, and the rate of descent of the metalimnion over the summer was slower. In the coldest year, 2003, stratification set up later and ended earlier and the mixed layer deepened more during cooling events than in the other three years. Increased rainfall caused two events with high stream discharge in 2003 with peak discharge 26 July and 13 August and three events in 2004 with peak discharge on 11 July, 19 July, and 01 August. The resulting intrusions caused the metalimnion to thicken after the first and third event in 2004. Mixed layer depths did not vary with k_d for which the mean and 95% confidence intervals were 0.73 $\pm$ 0.05 m^{-1}, 0.71 $\pm$ 0.05 m^{-1}, 0.60 $\pm$ 0.04 m^{-1}, and 0.50 $\pm$ 0.03 m^{-1} for the four years respectively.

The differences in surface forcing in the four years were subtle (Figs. 7-10). Maximum 30 minute averaged solar irradiance was typically 600-700 W m^{-2}, air temperatures varied between highs of 20^{o}C and lows of 0^{o}C, relative humidity ranged from 30% to 100%, and wind speeds had daily maxima ranging from 3 to ~10 m s^{-1}. Cold air masses, with decreased air temperatures and increased cloudiness and relative humidity, were present at least four times each summer in all years. Winds increased in magnitude and duration during cold fronts or during transitions between warm and cold air masses. Conditions during cold fronts in the first three years were relatively similar and differed from those in 2007. Cold temperatures persisted over day and night in the first three years, but in 2007 day time highs exceeded 10^{o}C whereas night time lows were near 0^{o}C. Cloud cover

reduced maximum daily solar radiation to values typically less than 200 W m^{-2} in the first three years; but maxima exceeded 200 W m^{-2} and were sometimes over 600 W m^{-2} in the first two cold fronts in 2007. Relative humidity was over 95% during cold fronts in the first three years but varied diurnally during 2007. Winds exceeded 5 m s^{-1} for at least a day prior to or during cold fronts in the first three years, but any increases in wind persisted for less than a day until the end of summer 2007. Wind directions tended to be persistently from the north or northwest during cold fronts in the first three years, but came from several directions in 2007 with often pronounced diel swings in direction during the event. Fluctuations in short wave radiation also set these years apart, with many more days having at least partial cloud cover in 2003, 2004, and 2006 than in 2007.

The magnitude of latent and sensible heat fluxes and net long wave radiation varied when warm and cold air masses were present (Fig. 7-10, F). When air temperatures exceeded surface water temperatures, sensible heat fluxes were positive (into the lake) and reached values as high as 125 W m^{-2}. Whenever air temperatures were colder than water temperatures, such as during cold fronts, sensible heat fluxes were negative (out of the lake) and had values as low as -150 W m^{-2}. When warm air masses were present, latent heat fluxes were less than -50 W m^{-2} early in the summer but increased with warming of surface waters. During cold fronts values dropped to lows of –100 W m^{-2} to - 150 W m^{-2} with the larger losses in warmer summers. Due to the typically greater cloud cover during cold fronts, heat losses from net long wave radiation tended to be less at those times than when warm air masses were present. However, conditions were sunny during two of the cold fronts in 2007 and net long wave radiation remained high, -100 W m^{-2}.

Surface heat fluxes, that is, the sum of latent and sensible heat fluxes and net long wave radiation, tended to be greater (more negative) during cold fronts than when warm air-masses were present and tended to be greater in warm than in cool years (Fig. 7-10, G). These patterns did not always hold. For instance, in 2004, surface heat fluxes at night in early summer were similar to or larger than those in the cold front which followed due to the low relative humidity which increased evaporation and the high net long wave radiation due to minimal cloud cover early that summer.

Effective heat flux, the sum of surface energy fluxes and net short wave radiation into the surface layer, determines whether the upper water column heats or cools (Figs 7-10G). The surface layer, or actively mixing layer, interacts directly with the atmosphere and is shallower than the epilimnion except when it deepens to the depth of the mixed layer during nocturnal cooling or during a cold front (Figs. 3B-6B, 3A-6A). Effective heat flux is negative at night because solar radiation is low. Whether values become positive or stay negative during the day depends upon the extent of cloud cover. During cold fronts with reduced solar radiation due to clouds, effective heat flux often remains negative or fluctuates between positive and negative values during the day. Thus during cold fronts, when the sum of the effective heat flux over several days is negative, the upper mixed layer cools and deepens (e.g., 13-18 July 2003 Figs. 3A,3B, 7G). In contrast, as the lake warms, the sum of the effective heat flux over many days is positive (e.g., 05-11 July 2003 Figs. 3A, 7G). Diurnal thermoclines form in the day due to the positive effective heat flux and erode at night when it becomes negative (Figs. 3A-6A). The magnitude and the variance in the values of maximum daily effective heat flux varied between years. Maximal daily values were higher in warmer years and fewer events occurred with negative effective heat flux in the day (Fig. 7G-10G).

Thus, the cooling and deepening of the mixed layer during cold fronts is muted in summers when surface water temperatures are warm as opposed to cool (Fig. 3A-6A).

The surface forcing which causes mixing is quantified as wind power, $P = \rho_{air} C_d U^3$ where ρ_{air} is density of air, C_d is a drag coefficient and U is wind speed, and buoyancy flux, B, which when negative indicates heat is being lost. $B = H^* g \alpha C_\rho^{-1} \rho^{-1}$ where H* is the effective heat flux, α is the coefficient of thermal expansion, C_p is specific heat capacity and ρ is density of water. Extended periods with high wind power occurred frequently in 2003 and occurred both when warm and cold air masses were present and buoyancy fluxes were respectively positive or negative (Fig. 11). Fewer events with high wind power occurred in the other years, and in 2007 they occurred only at the end of the study period. Buoyancy fluxes tended to transition from positive values at the beginning of summer to negative at the end with large negative values during cold fronts. As with the surface and effective heat fluxes, the maximal negative buoyancy fluxes were least in the coldest year. During all years, the upper water column became stratified when wind power was negligible and buoyancy flux was positive (Figs. 11, 3A-6A). If high wind power and positive buoyancy flux co-occurred, as in early 2003, the introduced heat could be mixed throughout the water column (Figs. 11A, 3A) and warming of the upper layers was minimal. Mixed layer deepening occurred in response to negative buoyancy fluxes.

The physical forcing quantified in Fig. 11 helps show why greater stability developed in warm as opposed to cool summers (Fig. 12A). Stability increased rapidly in 2004 and 2007 due to the positive buoyancy fluxes and low wind power early in the summer which caused heat to accumulate in the upper water column and increased the temperature difference between the upper and lower water column. Stability early in 2006 was lower as

buoyancy fluxes more quickly changed sign and wind power was slightly higher early in the season. Stability was least in 2003. Positive buoyancy fluxes in early summer 2003 were similar in magnitude to those in the warmer summers, but wind power was higher and the heat absorbed in the upper water column was mixed downwards. Stability varied throughout the summer in all years based on net heating and cooling; appreciable decreases occurred in response to cold fronts. Differences in diffuse light attenuation did not contribute to differences in stability because k_d was highest in 2003 when stability was least and lowest in 2007 when stability was greatest. The increased short wave into the lake in 2007 as opposed to the other years could have contributed to the increased surface temperatures and stability (Table 1). However, the sum of the surface energy fluxes was greatest in the hot summer such that they constituted a larger fraction of net short wave radiation than in the other years (Table 1). Over the 6 week period of our computations, less short wave energy was available to heat the lake in 2007 than in 2003 or 2004 and less heat accumulated over that interval. Thus, warmer surface water temperatures and greater stability do not depend upon incident short wave radiation. Instead they depend upon the sum of the net surface energy fluxes and net short wave radiation, and, as will be discussed in more detail later, the redistribution of heat within the lake. This redistribution caused lower stability in 2003 because heat was mixed downwards, not because less heat was introduced.

Turbulent kinetic energy produced by wind and surface cooling works against stratification to cause mixing. The flux of turbulent kinetic energy, F_q, was parameterized as $F_q = 1/2\ (w_*^3 + c_n^3 u_{*w}^3)$ which incorporates both the turbulence due to cooling, via the turbulent velocity scale for heat loss, w_*, and that due to shear stress via u_{*w}, with c_n a constant based on the different efficiencies of mixing from heat loss and wind (Fischer et al.

1979). F_q transitioned from high to low at intervals of three to ten days in the first 3 years and had maximum values of 10^{-6} m^3 s^{-3}. Maximum values of F_q were five times lower until the end of the study period in summer 2007. The ratio of F_q to stability was one to two orders of magnitude higher in the cold summer than in the hot summer, with values in the average and warm summer intermediate to the other two years and similar to each other (Fig. 12B). Maximum values in each year occurred after ice off and during cold fronts. Higher ratios are indicative of a higher proportion of turbulent kinetic energy for mixing relative to stratification.

L_N was higher in summers with warm and hot as opposed to cool surface temperatures (Figs. 3C-6C), and the frequency of events critical for formation of non-linear internal waves or upwelling decreased (Table 2). During 2003, the cold summer, L_N frequently dropped to 1 or lower and low values persisted for several days at a time. In 2004 and 2006, the warm and average years, values tended to be near 10 and dropped to values of 1 several times over the summer for a day or two. The decreases in L_N tended to occur when winds increased during the transitions between warm and cold air masses. In 2007, the hot summer, values were in excess of 10 for most of the summer and were only near 1 at the beginning and at the end of the summer. Wind speeds were similar in 2003, 2004, and 2006 (Figs. 7E-9E). The differences in L_N in those years thus resulted from the differences in stability of the lake which, as illustrated in Figs. 11-12, depends on the magnitude and phase of buoyancy flux and wind power.

The coefficient of eddy diffusivity in the metalimnion and hypolimnion increased as L_N decreased (Figs. 3B-6B). Thus, enhanced mixing, as indicated by K_z, occurred throughout more of the lower water column in 2003 than in 2004 and 2006. K_z was lower in

2007 than in other years. In all summers, K_z increased one to two orders of magnitude above molecular diffusivity when L_N dropped below 3 as typically occurred with the passage of fronts. In 2003, when the thickness of the metalimnion was on the order of 2 – 3 m, time scales of mixing across the metalimnion, $\tau_{mix} = l^2 / K_z$, were on the order of a few days (Table 2). When the metalimnion thickened to 3 m or more in 2004, 2006, and 2007, and L_N exceeded ~5, values of K_z equaled or were only slightly above the molecular conductivity of heat indicating turbulence was suppressed. With the thicker metalimnion, τ_{mix}, even when computed using relatively high values of K_z, was on the order of three weeks to months (Table 2). Several aspects of non-linear waves could change these estimates of mixing times. First, greater wave breaking can occur near sloping boundaries and increase K_z (MacIntyre et al. 1999); our calculation of τ_{mix}, by using relatively high values of K_z, takes this variation into account. Second, when non-linear waves form, the metalimnion can be compressed near lateral boundaries (Mortimer and Horn 1982; MacIntyre et al. in press) and thus locally reduce τ_{mix}. Analysis of the time series temperature data at CN station (Fig. 1) indicated that metalimnetic compression sufficient for transport on time scales of a few days occurred in 2006, the average year, but not in 2004 or 2007. Thus, the incidence of processes which could induce rapid fluxes between the upper and lower water column is reduced as average surface water temperatures become warmer.

Discussion

A warming trend was not detected in either summer air temperatures or mean epilimnetic temperatures at Toolik Lake (Fig. 2). The lack of a trend in air temperatures differs from the observations in summer at Barrow, Alaska, where muted increases in temperature were observed (Shulski and Wendler 2007), and likely reflects regional climate

variations. Meteorological data at Toolik Lake has primarily been collected during the positive phase of the Arctic Oscillation, and spatial analysis of summer temperature trends over the Arctic shows that temperatures in northern Alaska were not elevated in response to that oscillation as they were in other regions such as Siberia (Wang and Key 2003). Unlike Livingstone and Dokulil's (2001) results, mean epilimnetic temperatures in the lake were not significantly correlated with mean summer air temperatures (R^2=0.30, p< 0.21). In fact, surface water temperatures were ~ 1^{o}C below the mean in 1992 and ~1^{o}C above the mean in 2004, the two years with the warmest summer air temperatures (Fig. 2). Further, mean surface water temperatures were not correlated with downwelling solar radiation (R^2=0.19, p < 0.43) or mean wind speeds (R^2 = 0, p < 0.99). The lack of significant correlations and the high variance in surface water temperatures indicates that factors other than mean values of air temperature, solar radiation, and wind speed have a strong control on surface water temperatures and the associated mixing dynamics in the lake.

Fronts can increase turbulence in the water column by both increasing wind velocity and, as cold air masses move into a region, by increasing heat loss and convection at the air-water interface. This movement of air masses and associated increases in turbulence production may be a major factor influencing the surface water temperatures of lakes. The meteorological data in Figures 7 – 10 show higher, more persistent winds in summers with cold, average, and warm temperatures as opposed to the hot summer. Spectral analysis of the ten year wind record from the lake meteorological station confirms this pattern. All years have diel peaks in energy, but there was less energy at low frequencies in 2007 than in 2003 (Fig. 13A). This pattern held when spectra from 2007 and 1998, the two years with warmest surface water temperatures, were contrasted with spectra from other years (not shown). The

patterns held for w_*, u_*^2, and Fq. The spectra indicate that wind events occurring on time scales of 1.5 to 14 days were more energetic in summers with cool, average, and warm surface water temperatures than in those with hot temperatures.

The differences between years seen in the spectra are reinforced when we examine the interannual variability of frontal events in which strong winds or pronounced drops in temperature occur. The number of events, identified as mean wind speeds exceeding 5 m s^{-1} for 6 hours or air temperatures decreasing by 8^{o}C over 12 hours, was higher in summers with cooler as opposed to warmer surface water temperatures (Fig. 13B). Given the complex interactions between surface forcing and stratification (see below), we do not expect a simple linear relationship to exist between our event thresholds and surface temperature, and hence not all the variance is captured by linear regression ($R^2 = 0.3$, $p < 0.2$). Further, these metrics do not distinguish muted cold fronts that occur in summers with the warmest surface water temperatures when buoyancy fluxes are most negative and the flux of turbulent kinetic energy from cooling is highest. Despite these caveats, these results (Fig. 13B), obtained using the full meteorological record at Toolik Lake, support our inferences from the four representative years that mean summer epilimnetic temperatures were cooler in years with more wind events and frequent shifts between warm and cold air masses (Figs. 3-6, 11).

The phasing of warm or cold air masses relative to wind events as well as the persistence of these different air masses further distinguishes summers in which surface water temperatures were cold, average, warm and hot (Figs. 11, 12, 3-6). In 2003, the cold summer, winds were high when both warm and cold air masses were present and heat was mixed downwards leading to reduced heating of the upper layers, lower stability, lower L_N, and high K_z in the subsurface layer and metalimnion (13-19 July 2003). The mixing

dynamics in the lake were often in the low L_N regime. In 2004 and 2006, the warm and average summers, winds tended to be higher when cold air masses were present but not when warm ones were. The lower wind power when buoyancy fluxes were positive led to rapid heating in the upper layer, increased stability, and higher L_N for the same wind speeds as in cooler years. Thus, with low K_z at the base of the mixed layer, little heat was mixed downwards and turbulence was suppressed in the metalimnion (18-30 July 2004). Longer periods with positive heat flux induced a feedback in which heating led to further increases in L_N, less vertical mixing, and further accumulation of heat in the epilimnion. Thus, 2004 was a warmer summer than 2006. During cold fronts in those years, L_N were in the range to generate non-linear internal waves, and K_z increased, but with the thicker metalimnia the time scales for vertical fluxes were longer (Table 2). Summer 2007 had the warmest surface water temperatures because positive buoyancy fluxes were the highest and stayed high with low winds for an extended period in early summer. Stability increased rapidly, L_N rapidly increased to values of ~10, and turbulence at the base of the mixed layer was suppressed. Again the feedback loop was established in which persistent heating led to increased L_N, reduced K_z at the base of the mixed layer, and thus continued greater heat capture in the epilimnion. In this high L_N regime, convection from heat loss was the main driver of mixing, and because effective heat fluxes were positive in the day (Fig. 10G) convective heat loss occurred mainly at night and stratification was reestablished in the upper mixed layer each day. With persistent low to moderate winds and thus high L_N, surface temperatures stayed high until early August.

The extremes in surface water temperatures and mixing dynamics in 2007 and 2003 resulted from persistent warm air masses or high winds early in the ice free period. As

discussed above, the persistent, high buoyancy fluxes and low winds in early summer 2007 led to the enhanced stratification and high L_N regime in that year. In the cold summer of 2003, conditions were windy for approximately two weeks in early summer (28 Jun – 9 July) despite positive buoyancy flux. Consequently, stratification was weak (Fig. 3A, 6, 11) and considerable mixed layer deepening was possible in the cold front which followed (13 – 18 July 2003). Other aspects of the surface meteorology combined with critical aspects of the physical limnology of arctic lakes further contributed to the differences between the two extreme years. Because heat losses from evaporation are low in arctic lakes relative to warmer water bodies (MacIntyre and Melack 2009), mixed layer deepening requires persistent cloudy conditions during cold fronts in order to reduce or prevent restratification in the day. Moderate to high winds must persist for longer than a day. While cold air masses moved over the lake seven times in each of the two summers, conditions at those times were quantitatively different. In 2007, air temperatures, relative humidity, and winds varied over the course of a day whereas conditions during cold fronts in 2003 were stable for longer periods. Higher winds came only from the south in 2007 as opposed to from both northerly and southerly directions in 2003. Temperatures were persistently much colder towards the end of summer in 2003 than in 2007 as well as in the other summers. With the higher irradiance in 2007, effective heat flux was greater in the day despite cloudy conditions. Thus, the summers with the extremes in surface water temperatures and mixing dynamics differed not only with respect to persistence of warm and cold air masses but also in the conditions present during cold fronts.

The among-year differences in epilimnetic temperatures and mixing dynamics at Toolik Lake likely depend upon large scale circulation patterns (circulation patterns

described in Maslanik et al. 2007; Serreze and Barrett 2008) and regional scale factors which influence the generation of fronts (Lynch et al. 1999; 2001). Summers with anomalously strong arctic synoptic activity correspond to positive northern annular mode (NAM; also known as the Arctic Oscillation (AO)) conditions and anomalous low pressure over the Arctic (Serreze and Barrett (2008), their Figs. 12-15). Northwesterly winds transport cold air over northern Alaska. As Serreze and Barrett (2008) point out, however, the connection between synoptic activity and the AO is not always robust. We find that the AO index is not coherent with air or surface water temperatures at Toolik (analysis not shown) and recognize that other large-scale circulation patterns are at play in the arctic sector (Maslanik et al. 2007). We do find, however, a consistent connection to the large-scale circulation. In all years for which meteorological data were collected on the lake, the strongest winds came from the south, but in the years with cold surface water temperatures (e.g., the summers of 2000-2003) the winds had an anomalously northerly component, with low sea-level pressure near the Alaskan coast (analysis not shown). We hypothesize that the mixing dynamics within Toolik Lake are highly dependent upon whether high or low pressure is found near the Alaskan coast, with limited mixing and low connectivity between the upper and lower water column ($L_N > 10$) in summers when high pressure is to the north and increased mixing ($L_N < 10$) when low pressure is to the north.

It is uncertain how the frontal activity which affects mixing dynamics in Toolik Lake will vary with climate change. Synoptic eddy activity in the atmosphere, and the associated cold front events, are strongly controlled by north-south temperature contrasts and the strength of the stable stratification of air in the troposphere (Serreze et al. 2001; Serreze and Barrett 2008). We expect that on the largest scale, polar amplification of surface warming

will weaken the temperature contrast between high and low latitudes. However, the greater warming over land than ocean in summer will maintain or locally strengthen the north-south temperature gradient between the Alaskan coast and the Arctic Ocean which can drive north to south advective flows. Most climate models predict strong surface trapping of the heating, which corresponds to a reduction of the Arctic thermal inversion and hence of tropospheric stratification, conditions which would lead to less frontogenesis, but there is now ongoing discussion about whether this surface trapping effect is realistic (Graversen et al. 2008; Thorne 2008; Boé al. 2009). Given these complexities, there is an insufficient basis at this point to predict future frontal activity in northern Alaska. A conservative conclusion would be that, given the lack of trends in synoptic activity to this point (Serreze and Barrett 2008), there will likely be no significant trend in synoptic activity in the coming few decades, suggesting that epilimnetic temperatures and mixing dynamics at Toolik will not exhibit significant trends either.

Both traditional analyses and dimensionless indices can be used to relate mean summer epilimnetic temperatures to mixing dynamics for the full record of lake temperature data and to assess future scenarios. Mean lake temperature and stability of the lake are strongly correlated with mean surface temperatures (Fig. 14A: $R^2 = 0.91$, $p < 0.05$, B: $R^2 = 0.92$, $p < 0.05$). The mean stability in the two warmest years is over 30% higher than in any other year. Log-averaged L_N also depends upon lake temperature (Fig. 14C: $R^2 = 0.67$, $p < 0.05$). Based on our analysis of the high resolution data, we infer that throughout the period of record the connectivity between the upper and lower depths of the lake has varied with mean summer temperature in predictable ways. That is, when mean epilimnetic temperatures are less than 10.5^{o}C, vertical fluxes of heat, solutes, and particulates from upwelling and due

to the breaking of non-linear internal waves will occur ~15 times each summer (Table 2). The mixing dynamics of the lake will be in the low L_N regime. When mean epilimnetic temperatures are between 10.5°C and 13.5°C, upwelling events will be infrequent and turbulence will be produced by instabilities in the internal wave field. Vertical fluxes further depend upon the thickness of the metalimnion (Table 2). Mixing dynamics will be in the intermediate L_N regime. A tipping point is reached when meteorological forcing is similar to that in 2007 when mean epilimnetic temperatures equal or exceed 14°C, the stability of the lake reaches ~80 J m^{-2}, and log-averaged values of L_N exceed ~10 such that only cooling can induce vertical fluxes. Mixing dynamics will be in the high L_N regime. Under those conditions connectivity between the upper and lower water column is considerably reduced, and arctic lakes behave similarly to lakes in the temperate zone in which non-linear waves are only observed in autumn in the larger lakes and not at all in the small ones (Thorpe 1974; Horn et al. 2001; MacIntyre and Melack 2009). Based on our assessment of factors influencing arctic climate, we anticipate this relation between mean epilimnetic temperatures and L_N will hold and will help predict future conditions at Toolik Lake.

The linkages established here between large scale atmospheric forcing, mixing dynamics, and mean summer surface temperatures in one arctic lake enable us to generalize to other lakes. We argue that frontal activity exerts a strong control on lake temperatures and mixing dynamics. In the absence of significant trends in this activity (Serreze and Barrett 2008), summer temperatures in stratified, Alaskan arctic lakes similar in size to Toolik will primarily remain cool to warm, and vertical fluxes will continue to be induced by upwelling and instabilities of non-linear internal waves. Occasionally, frontal activity will be less and mixing will be reduced (L_N >10). Some small (~0.1 km^2), stratified lakes near Toolik Lake

have similar dynamics, but smaller lakes with lesser fetch are already in a state in which $L_N >$ 10 for most of the summer. If increased warming occurs in arctic springs (Wang and Key 2003), small lakes that are relatively deep (>5 m) might forego spring mixing (Parsons-Field 2008). Temperatures in shallow, unstratified lakes may be tied more closely to air temperatures than deeper, stratified lakes such as Toolik. In the high arctic or at high elevation, warming may melt permanent ice-cover and allow mixing to occur, while ice-free lakes now too cold to reach 4°C and stratify may warm sufficiently to maintain stratification during summer (Kling 2009). In regions such as low-arctic Siberia, where temperature regimes in the past may have been like those at Toolik but where the positive phase of the Arctic Oscillation augmented summer air temperatures in the recent past (Wang and Key 2003), some of the deeper lakes may have transitioned to regimes with $L_N > 10$. We suggest that the future mixing dynamics of these other arctic lakes will also be tightly coupled to large-scale atmospheric circulation patterns and frontal activity as it is affected by conditions on land and over the ocean (Lynch et al. 1999, 2001; Maslanik et al. 2007).

References

Boé J., A. Hall, and X .Qu. In press. Current GCMs' unrealistic negative feedback in the Arctic. J. Climate.

Boegman, L., G. N. Ivey, and J. Imberger. 2005. The degeneration of internal waves in lakes with sloping topography. Limnol. Oceanogr. **50**: 1620-1637.

Bonsal, B. B., T. D. Prowse, C.R. Duguay, and M. P. Lacroix. 2006. Impacts of large-scale teleconnections on freshwater-ice break/freeze-up dates over Canada. J. Hydrol. **330**: 340-353.

Evans, M. A., S. MacIntyre, and G. W. Kling. 2008. Internal wave effects on photosynthesis: experiments, theory, and modeling. Limnol. Oceanogr. **53** :339-353.

Fischer, H. B., E. J. List, R. C. Y. Koh, J. Imberger, and N. H. Brooks. 1979. Mixing in inland and coastal waters. Academic Press.

Graverson, R. G., T. Mauritsen, M. Tjernstrom, E. Kallen, and G. Svensson. 2008. Vertical structure of recent Arctic warming. Nature **541**: 53-56.

Hinzman, L. D., N. D. Bettez, W. R. Bolton, F. S. Chapin, M. B. Dyurgerov, C. L. Fastie, B. Griffith, R. D. Hollister, A. Hope, H. P. Huntington, A. M. Jensen, G. J. Jia, T. Jorgenson, D. L. Kane, D. R. Klein, G. Kofinas, A. H. Lynch, A. H. Lloyd, A. D. McGuire, F. E. Nelson, W. C. Oechel, T. E. Osterkamp, C. H. Racine, V. E. Romanovsky, R. S. Stone, D. A. Stow, M. Sturm, C. E. Tweedie, G. L. Vourlitis, M. D. Walker, D. A. Walker, P. J. Webber, J. M. Welker, K.S. Winker, and K. Yoshikawa. 2005. Evidence and implications of recent climate change in northern Alaska and other arctic regions. Climatic Change **72**: 251-298.

Horn, D. A., J. Imberger, and G. N. Ivey. 2001. The degeneration of large-scale interfacial gravity waves in lakes. J. Fluid Mech. **434**:181-207.

Idso, S. 1973. On the concept of lake stability. Limnol. Oceanogr. **18**: 681-683.

Imberger, J. 1985. The diurnal mixed layer. Limnol. Oceanogr. **30**: 737-770.

Imberger, J., and J. C. Patterson. 1990. Physical limnology. Advances in applied mechanics **27**: 303-475.

Jassby, A., and T. M. Powell. 1975. Vertical patterns of eddy diffusion during stratification in Castle Lake, California. Limnol. Oceanogr. **20**: 530-543.

Kalff, J. 2001. Limnology. Prentice Hall.

Kling, G. W. 2009. Lakes of the Arctic, p. 577-588. *In* Gene E. Likens [ed.], Encyclopedia of inland waters. Elsevier.

Lewis Jr., W. M., 1973. The thermal regime of Lake Lanao (Philippines) and its theoretical implications for tropical lakes. Limnol. Oceanogr. **18**: 200-217.

Livingstone, D. M., and M. T. Dokulil. 2001. Eighty years of spatially coherent Austrian lake surface temperatures and their relationship to regional air temperature and the North Atlantic Oscillation. Limnol. Oceanogr. **46**: 1220-1227.

Lynch, A. H., G. B. Bonan, F. S. Chapin III, and W. Wu. 1999. Impact of tundra ecosystems on the surface energy budget and climate of Alaska. J. Geophys. Res. **104**: 6647-6660.

Lynch, A. H., A. G. Slater, and M. Serreze. 2001. The Alaskan arctic frontal zone: Forcing by orography, coastal contrast, and the boreal forest. J. Clim. **14**: 4351-4362.

MacIntyre, S. 1993. Mixing in the euphotic zone of a shallow, turbid lake: Consequences for the phytoplankton. Limnol. Oceanogr. **38**: 798-817.

MacIntyre, S., K. M. Flynn, R. Jellison, and J. R. Romero. 1999. Boundary mixing and nutrient flux in Mono Lake, CA. Limnol. Oceanogr. **44**:512-529.

MacIntyre, S., J. R. Romero, and G.W. Kling. 2002. Spatial-temporal variability in mixed layer deepening and lateral advection in an embayment of Lake Victoria, East Africa. Limnol. Oceanogr. **47**: 656-671.

MacIntyre, S., J. O. Sickman, S. A. Goldthwait, and G. W. Kling. 2006. Physical pathways of nutrient supply in a small, ultra-oligotrophic lake during summer stratification. Limnol. Oceanogr. **51**: 1107-1124.

MacIntyre, S., and J. M. Melack. 2009. Mixing dynamics in lakes across climatic zones. p. 603-612. *In* G. E. Likens. [ed]., Encyclopedia of inland waters. Elsevier.

MacIntyre, S., J. F. Clark, R. Jellison, and J. P. Fram. (in press). Turbulent mixing induced by nonlinear internal waves in Mono Lake, California. Limnol. Oceanogr.

Maslanik, J. S., Drobot, C. Fowler, W. Emery, and R. Barry. 2007. On the Arctic climate paradox and the continuing role of atmospheric circulation in affecting sea ice conditions. Geophys. Res. Letters. **34**: L03711, doi:10.1029/2006GL028269.

McDonald, M. E., A. E. Hershey, and M. C. Miller. 1996. Global warming impacts on lake trout in arctic lakes. Limnol. Oceanogr. **41**: 1102-1108.

Miller, M. C., P. Spatt, P. Westlake, D. Yeakel and G. R. Hater. 1986. Primary production and its control in Toolik Lake, Alaska. Arch. Hydrobiol. Suppl. **74**: 97-131.

Monahan, A. H. 2006. The probability distribution of sea surface wind speeds. Part I: Theory and sea winds observations. J. Climate **19**: 497-520.

Monismith, S. G. 1986. An experimental study of the upwelling response of stratified reservoirs to surface shear stress. J. Fluid Mech. **171**: 407-439.

Mortimer, C. H., and W. Horn. 1982. Internal wave dynamics and their implications for plankton biology in the Lake of Zurich. Vier. Natur. Gesell. Zurich. **127**: 299-318.

O'Brien, W. J., M. Bahr, A. E. Hershey, J. E. Hobbie, G. W. Kipphut, G. W. Kling, H. Kling, M. McDonald, M. C. Miller, P. Rublee, and J. R. Vestal. 1997. The limnology of Toolik Lake. p. 61-106. *In* A. M. Milner and M. W. Oswood [eds.], Alaskan freshwaters. Springer-Verlag.

Overland, J. E., M. C. Spillane, and N. N. Soreide. 2004. Integrated analysis of physical and biological pan-Arctic change. Climatic Change **63**: 291-322.

Parsons-Field, A. 2008. Winter conditions and spring convection in Toolik Lake, Alaska. M.S. thesis. University of California at Santa Barbara.

Saggio, A., and J. Imberger. 1998. Internal wave weather in a stratified lake. Limnol. Oceanogr. **43**: 1780-1795.

Serreze, M. C., and A. P. Barrett. 2008. The summer cyclone maximum over the central Arctic Ocean. J. Clim. **21**: 1048-1065.

Serreze, M. C., J. E. Walsh, F. S. Chapin III, T. Osterkamp, M. Dyurgerov, V. Romanovsky, W.C. Oechel, J. Morison, T. Zhang, and R.G. Barry. 2000. Observational evidence of recent change in the northern high-latitude environment. Climatic Change **46**: 159-207.

Serreze, M. C., A. H. Lynch, and M. P. Clark. 2001. The arctic frontal zone as seen in the NCEP-NCAR reanalysis. J. Clim. **14**: 1550-1567.

Shulski, M., and G. Wendler. 2007. The climate of Alaska. Univ. of Alaska Press.

Talling, J. F. 1966. The annual cycle of stratification and phytoplankton growth in Lake Victoria (East Africa). Int. Rev. Gesamten Hydrobiol. **51**: 545-621.

Tennekes, H., and J. L. Lumley. 1972. A first course in turbulence. MIT Press.

Thompson, D. W. J., and J. M. Wallace. 2001. Regional climate impacts of the Northern Hemisphere Annular Mode. Science. **293**: 85-89.

Thorne, P. W. 2008. Arctic tropospheric warming amplification? Nature **455:** E1-E2 doi: 10.1038/nature07256.

Thorpe, S. A. 1974. Near-resonant forcing in a shallow two-layer fluid: a model for the internal surge in Loch Ness? J. Fluid Mech. **63**: 509-527.

Vincent, W. F., S. MacIntyre, R. H. Spigel, and I. Laurion. 2008. Physical limnology of high-latitude lakes. p. 65-81. *In* W. F. Vincent and J. Laybourne-Parry [eds.], Polar limnology. Oxford Univ. Press.

Wang, X. and J. R. Key. 2003. Recent trends in arctic surface, cloud, and radiation properties from space. Science **299**: 1725-1728.

Yeates, P. S., and J. Imberger. 2004. Pseudo two-dimensional simulations of internal and boundary fluxes in stratified lakes and reservoirs. Intl. J. River Basin Management **1**: 297-319.

Table 1. Sum of net short wave radiation SWnet; sum of surface energy fluxes (Srfflx) divided by SWnet; potential heat storage (PHS) for the main basin computed as (1-Srfflx) x SWnet; and heat stored within the main basin. Computations are for the interval from 29 June to 18 August.

Year[+]	SWnet ($W\ m^{-2}$)	Srfflx/ SWnet (%)	PHS ($W\ m^{-2}$)	Heat stored (J)
2003	2.1×10^6	61.6	7.9×10^5	8.2×10^7
2004	2.3×10^6	72.5	6.2×10^5	8.1×10^7
2007	3.1×10^6	77.6	6.9×10^5	5.5×10^7

[+]2006 was not included in the analysis due to missing long wave radiation for part of the summer.

Table 2. Number of events with $L_N <= 1$ and with $1 < L_N <= 3$; metalimnetic thickness l mid-lake during cold fronts; and time for cross-metalimnetic mixing, τ_{mix}, assuming $^{\dagger}K_z = 10^{-5}$ m^2 s^{-1} and $*K_z = 10^{-6}$ m^2 s^{-1} for the four study years. Events were defined when L_N averaged over 8 hours dropped below the threshold with the further criterion that no more than one event can occur every two days.

Year (conditions)	2003 (cold)	2004 (warm)	2006 (average)	2007 (hot)
$L_N < 1$	17	2	4	1
$1 < L_N < 3$	3	7	15	6**
l (m)	2-3	4-5	3-4	5
$^{\dagger}\tau_{mix}$ (days)	4-10 days	18-30 days	10-18 days	30 days
$*\tau_{mix}$ (days)	46 - 104	185 - 290	104-185	290

** But only at beginning and end of study period.

Figure Captions

Figure 1. Bathymetric map of Toolik Lake showing the major basins within the lake and the location of the meteorological station and the thermistor arrays at Toolik Main (TM) and the Central station (CN). Exact locations varied slightly each year.

Fig 2. (A) Time series of mean temperatures at 2 m depth computed from temperature profiles (boxes) taken in Toolik Lake from 1975 to 2008 and from a thermistor (closed circle) moored at 2 m depth beginning in 1990. 95% confidence intervals are shown for the profile data. The longer trend line is for the profile data. The dashed line is from McDonald et al. (1996). (B) Time series of mean air temperatures from the meteorological station on land from 1989 - 2007. Averages for both time series are computed from 19 June – 23 August.

Fig. 3. Time series of (A) isotherms, (B) the coefficient of eddy diffusivity, K_z, and depth of the actively mixing layer (black line), and (C) Lake numbers measured at Toolik Main in 2003. Asterisks to the left in the upper panel indicate depths of thermistor arrays. The color scale for K_z is restricted to 10^{-3} to 10^{-7} m^2 s^{-1} so that changes in turbulence in the meta- and hypolimnion can be discerned. K_z in the actively mixing layer is typically 10^{-2} m^2 s^{-1}.

Fig. 4. As in Figure 3 but for 2004.

Fig. 5. As in Figure 3 but for 2006.

Fig. 6. As in Figure 3 but for 2007.

Fig 7. Time series of (A) short wave radiation, (B) air (line) and surface water (dashed line) temperatures, (C) relative humidity, (D) wind direction, (E) wind speed, (F) sensible (dotted line) and latent (gray line) heat fluxes and net long wave radiation (black line), and (G) surface energy fluxes (gray line) and effective heat flux (solid line) for 2003. Data are presented as 30 minute averages.

Fig. 8. As in Figure 7 but for 2004.

Fig. 9. As in Figure 7 but for 2006.

Fig. 10. As in Figure 7 but for 2007.

Fig. 11. Time series of daily averaged wind power (black line, W m^{-2}) and buoyancy flux x 10^7 (gray line, m^2 s^{-3}) for all 4 years.

Fig. 12. (A) Time series of stability (J m^{-2}) and (B) ratio of daily averaged Fq to stability (m^2 $kg^{-1}s^{-1}$) for the 4 years.

Fig. 13. (A) Power spectra and 95% confidence limits of wind speed (WS) in 2003 and 2007. Results from all years of lake data also show low energy at frequencies less than a day ($<10^{-5}$ Hz) for the other very warm year and higher energy at lower frequencies in other years, (B)

Number of events with mean winds > 5 m s for 6 hours or with cooling exceeding 8^{o}C over 12 hours from 1990-2007.

Fig. 14. Relation between mean epilimnetic temperatures and (A) mean lake temperatures and (B) stability from 1975 to 2007 and (C) log-averaged Lake numbers from 1998 – 2000 and from 2002 - 2008.

Fig. 1

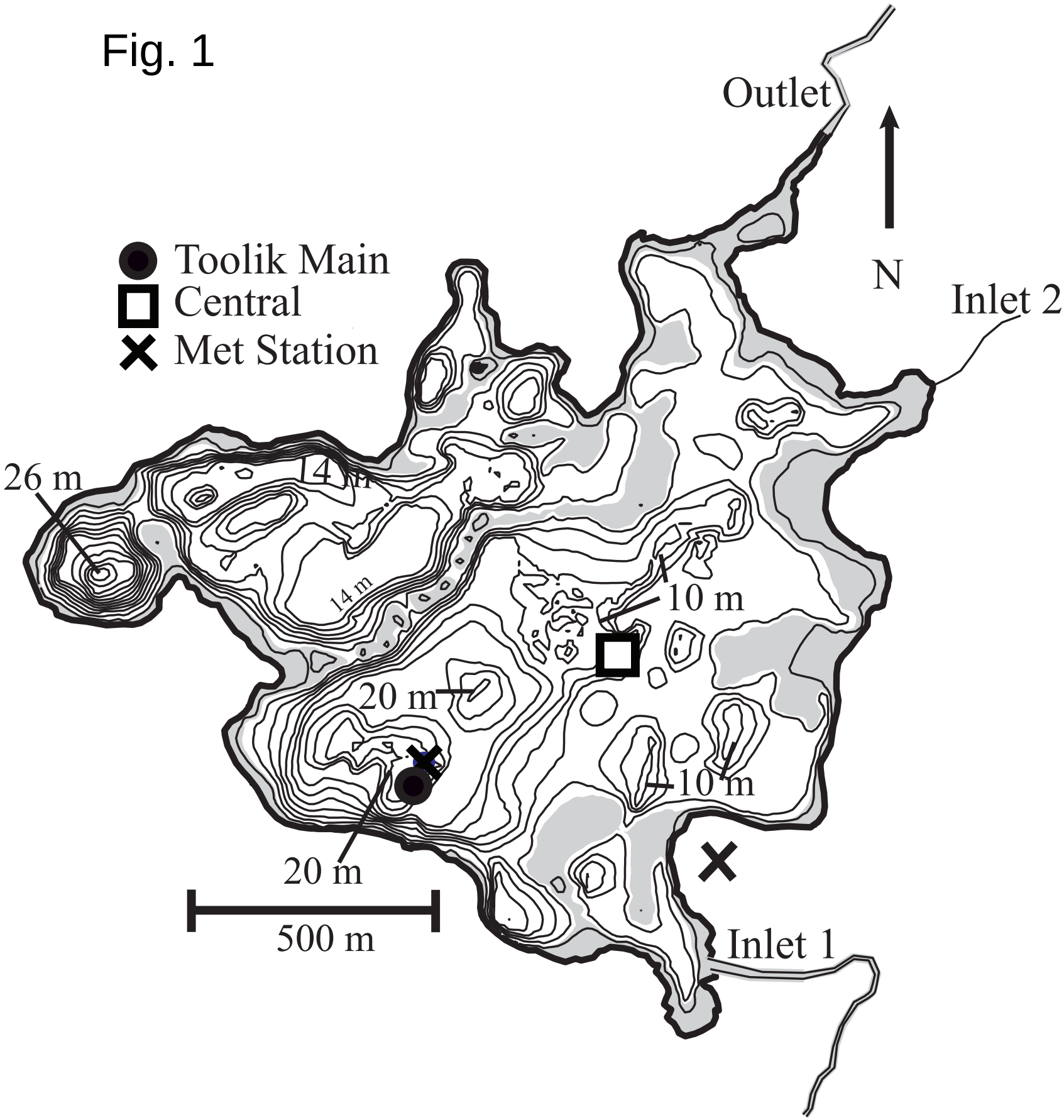
Outlet
N
Inlet 2
Toolik Main
Central
Met Station
26 m
14 m
14 m
10 m
20 m
10 m
20 m
500 m
Inlet 1

Fig. 2

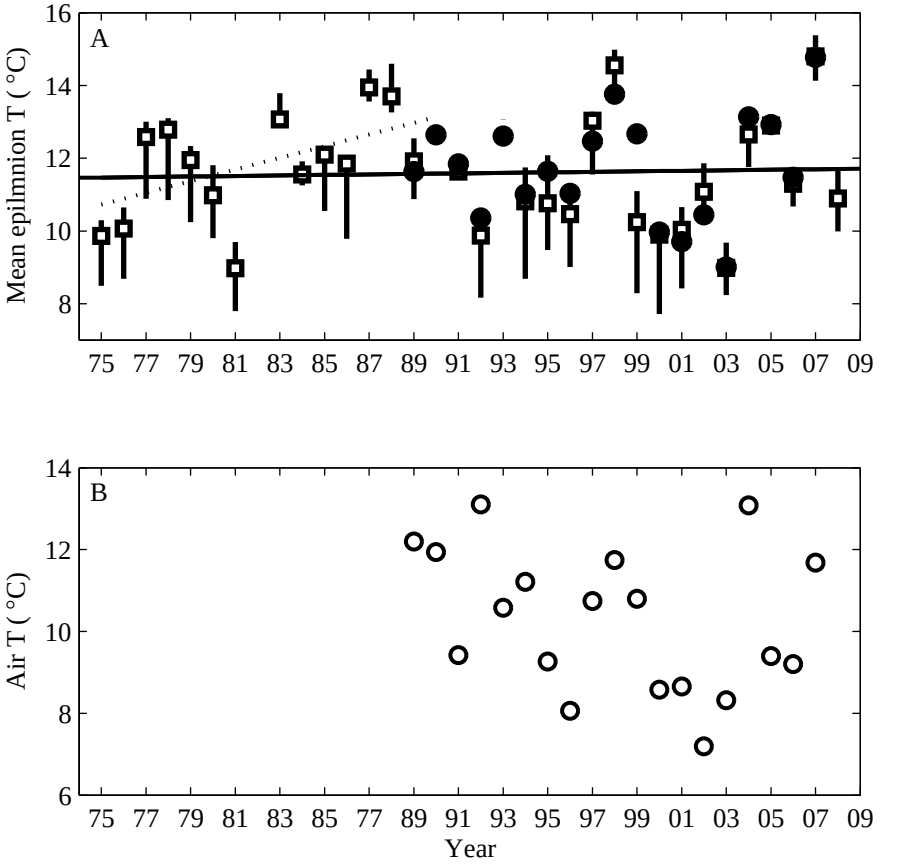
A
Mean epilmnion T (°C)
16
14
12
10
8
75 77 79 81 83 85 87 89 91 93 95 97 99 01 03 05 07 09
B
Air T (°C)
14
12
10
8
6
75 77 79 81 83 85 77 89 91 93 95 97 99 01 03 05 07 09
Year

Fig. 3

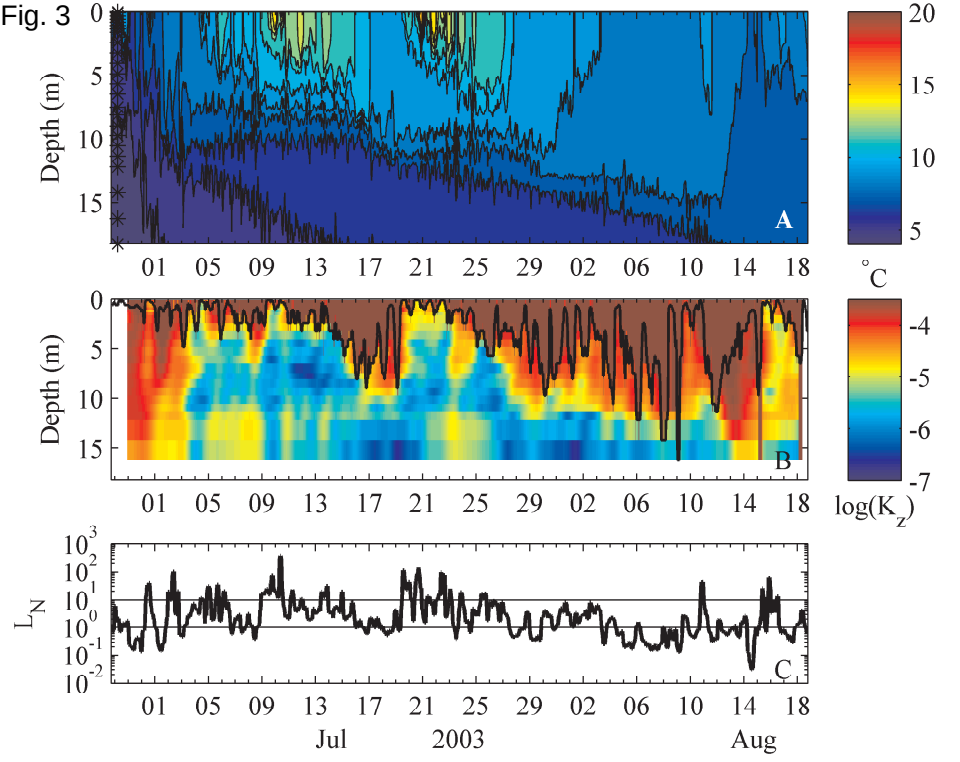
Depth (m)
0
5
10
15
A
20
15
10
5
°C
01 05 09 13 17 21 25 29 02 06 10 14 18
Depth (m)
B
-4
-5
-6
-7
log(K_z)
L_N
10^3
10^2
10^1
10^0
10^-1
10^-2
C
Jul
2003
Aug

Fig. 4

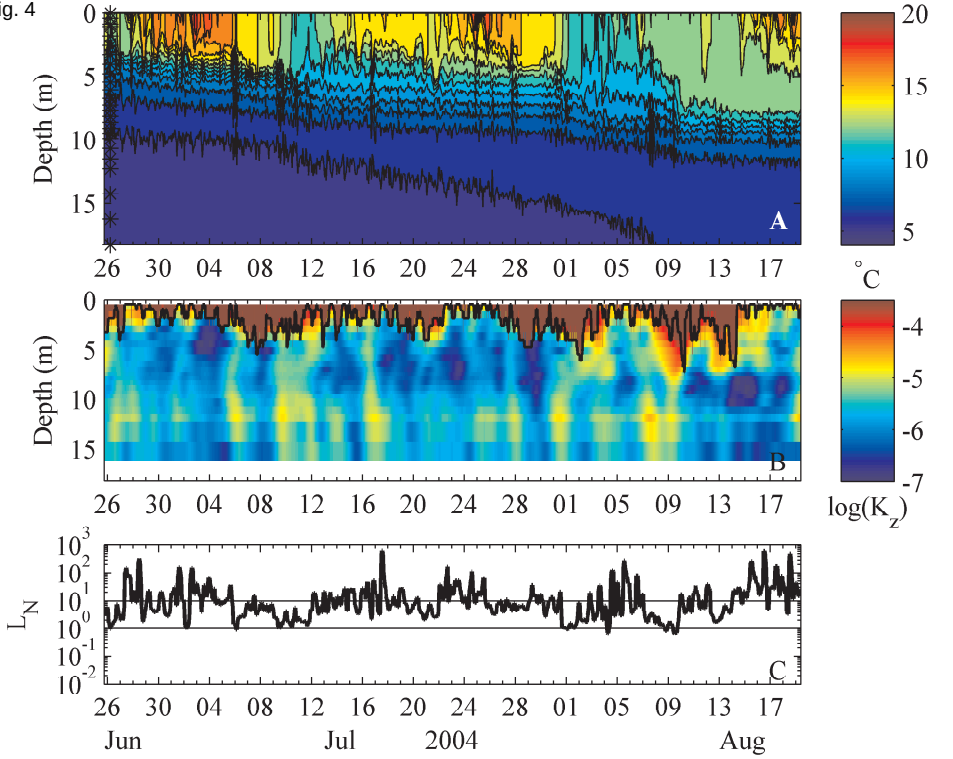
Depth (m)
0
5
10
15
A
20
15
10
5
°C
26 30 04 08 12 16 20 24 28 01 05 09 13 17
Depth (m)
B
-4
-5
-6
-7
log(K_z)
L_N
C
Jun
Jul
2004
Aug

Fig. 5

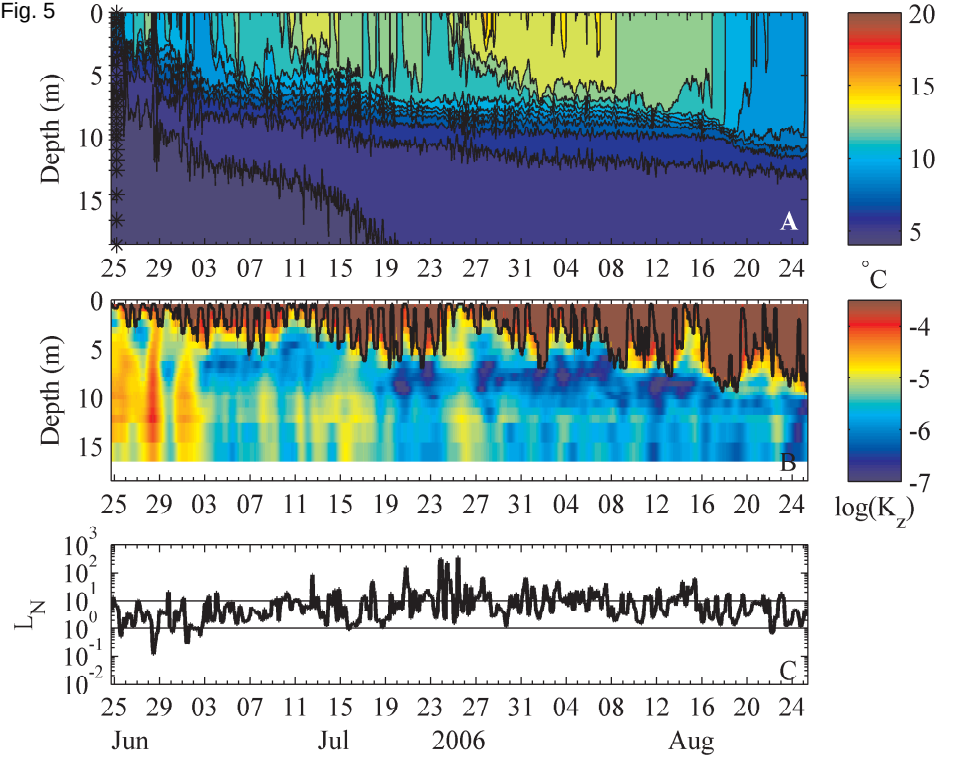
Depth (m)
0
5
10
15
A
20
15
10
5
°C
25 29 03 07 11 15 19 23 27 31 04 08 12 16 20 24
Depth (m)
B
-4
-5
-6
-7
log(K_z)
L_N
10^3
10^2
10^1
10^0
10^-1
10^-2
C
Jun
Jul
2006
Aug

Fig. 6

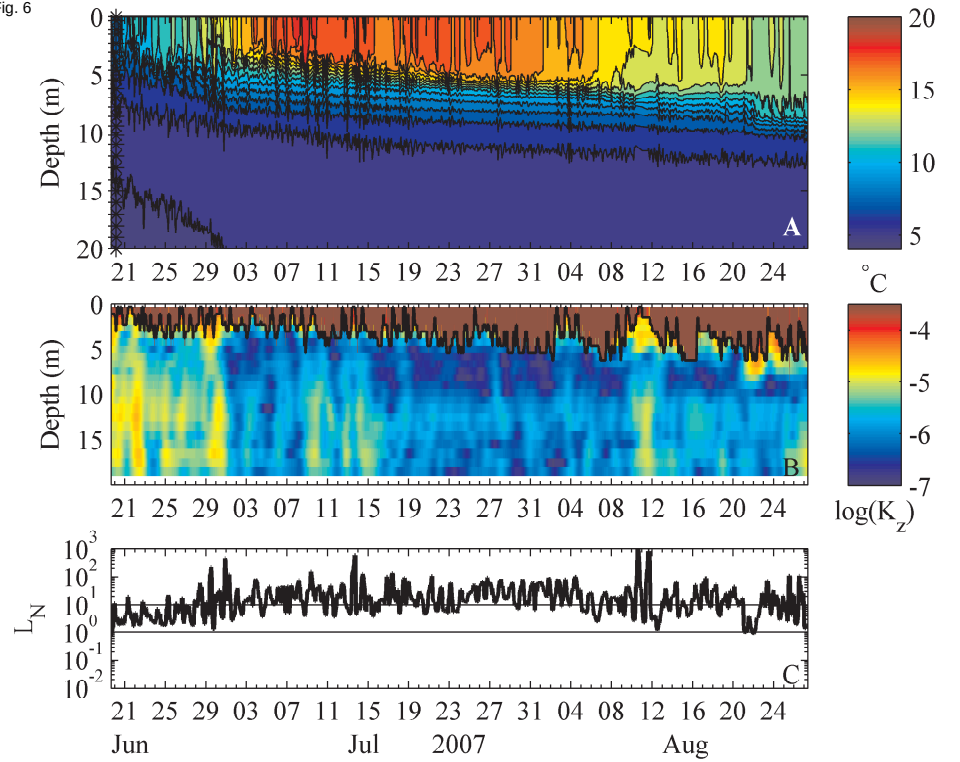
Depth (m)
0
5
10
15
20
A
21 25 29 03 07 11 15 19 23 27 31 04 08 12 16 20 24
20
15
10
5
°C
Depth (m)
0
5
10
15
B
21 25 29 03 07 11 15 19 23 27 31 04 08 12 16 20 24
-4
-5
-6
-7
log(K_z)
L_N
10^3
10^2
10^1
10^0
10^-1
10^-2
C
21 25 29 03 07 11 15 19 23 27 31 04 08 12 16 20 24
Jun
Jul
2007
Aug

Fig. 7

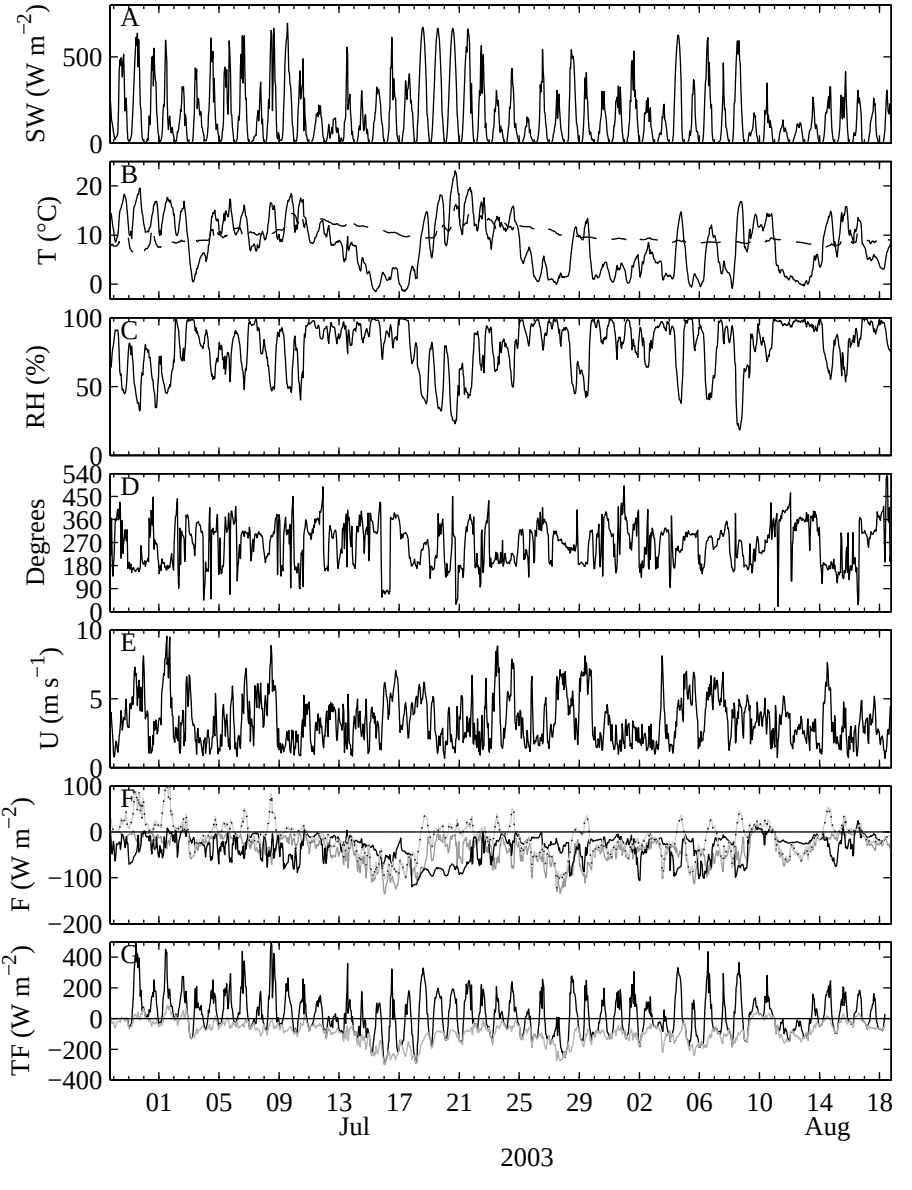
A
SW (W m^{-2})
500
0
B
T (°C)
20
10
0
C
RH (%)
100
50
0
D
Degrees
540
450
360
270
180
90
0
E
U (m s^{-1})
10
5
0
F
F (W m^{-2})
100
0
−100
−200
G
TF (W m^{-2})
400
200
0
−200
−400
01
05
09
13
17
21
25
29
02
06
10
14
18
Jul
Aug
2003

Fig. 8

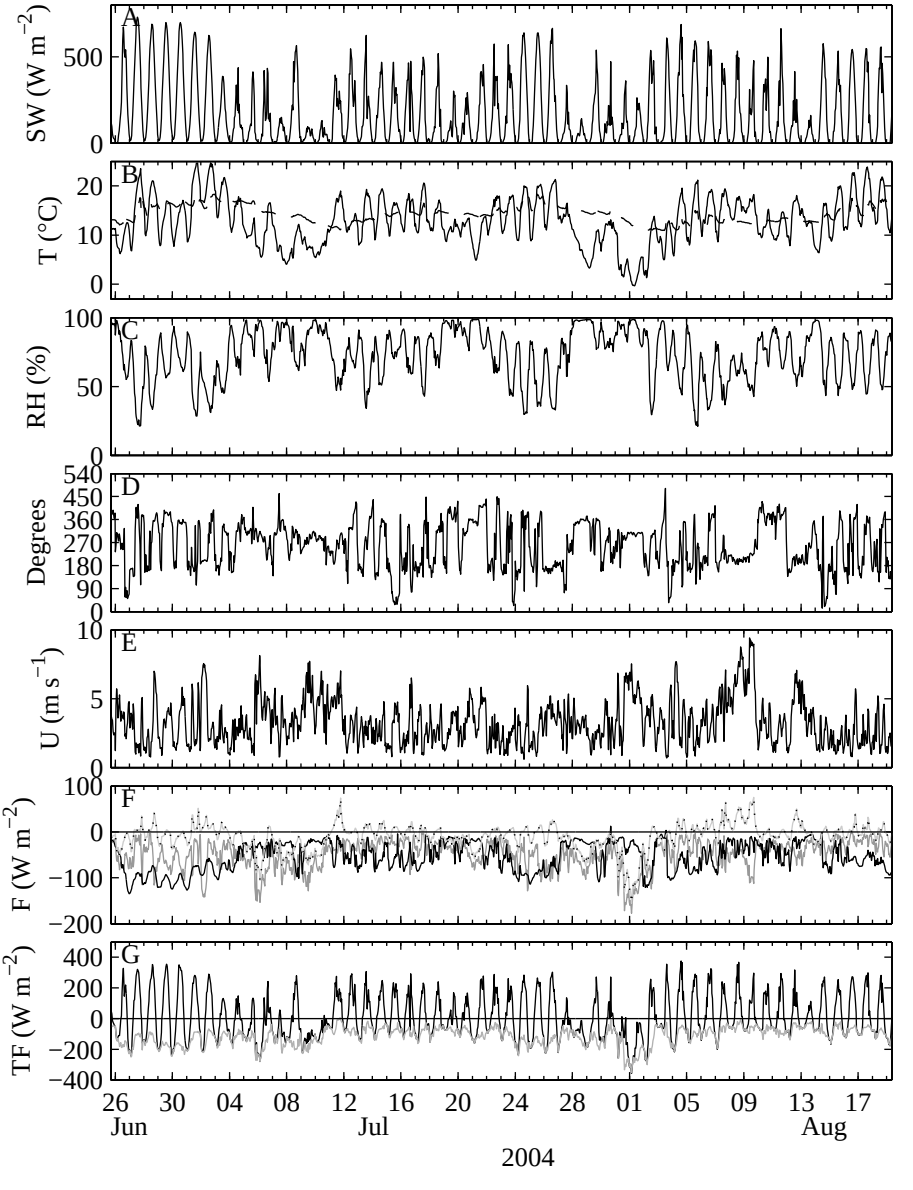
A
SW (W m^{-2})
500
0
B
T (°C)
20
10
0
C
RH (%)
100
50
0
D
Degrees
540
450
360
270
180
90
0
E
U (m s^{-1})
10
5
0
F
F (W m^{-2})
100
0
−100
−200
G
TF (W m^{-2})
400
200
0
−200
−400
26 30 04 08 12 16 20 24 28 01 05 09 13 17
Jun
Jul
Aug
2004

Fig. 9

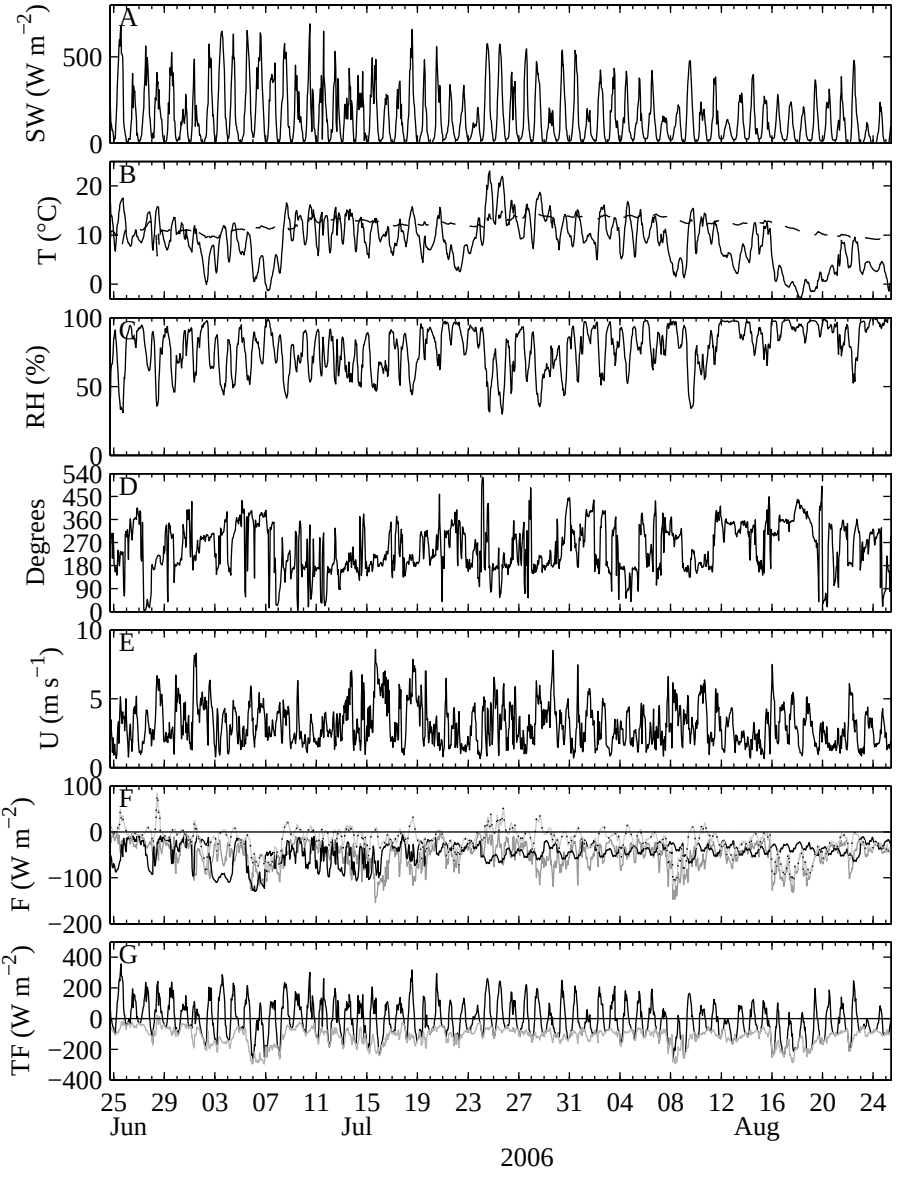
A
SW (W m^{-2})
500
0
B
T (°C)
20
10
0
C
RH (%)
100
50
0
D
Degrees
540
450
360
270
180
90
0
E
U (m s^{-1})
10
5
0
F
F (W m^{-2})
100
0
−100
−200
G
TF (W m^{-2})
400
200
0
−200
−400
25 29 03 07 11 15 19 23 27 31 04 08 12 16 20 24
Jun
Jul
Aug
2006

Fig. 10

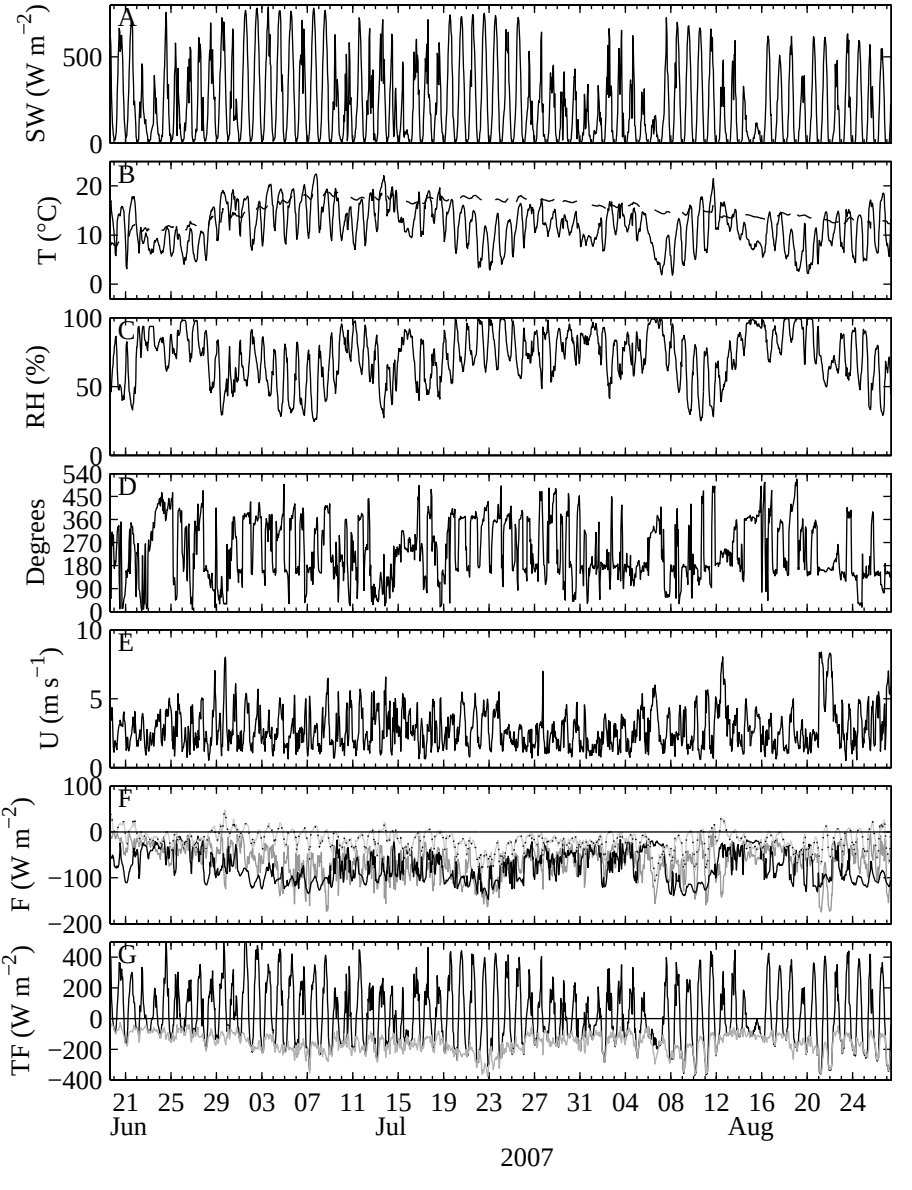
A
SW (W m^{-2})
500
0
B
T (°C)
20
10
0
C
RH (%)
100
50
0
D
Degrees
540
450
360
270
180
90
0
E
U (m s^{-1})
10
5
0
F
F (W m^{-2})
100
0
−100
−200
G
TF (W m^{-2})
400
200
0
−200
−400
21 25 29 03 07 11 15 19 23 27 31 04 08 12 16 20 24
Jun
Jul
Aug
2007

Fig. 11

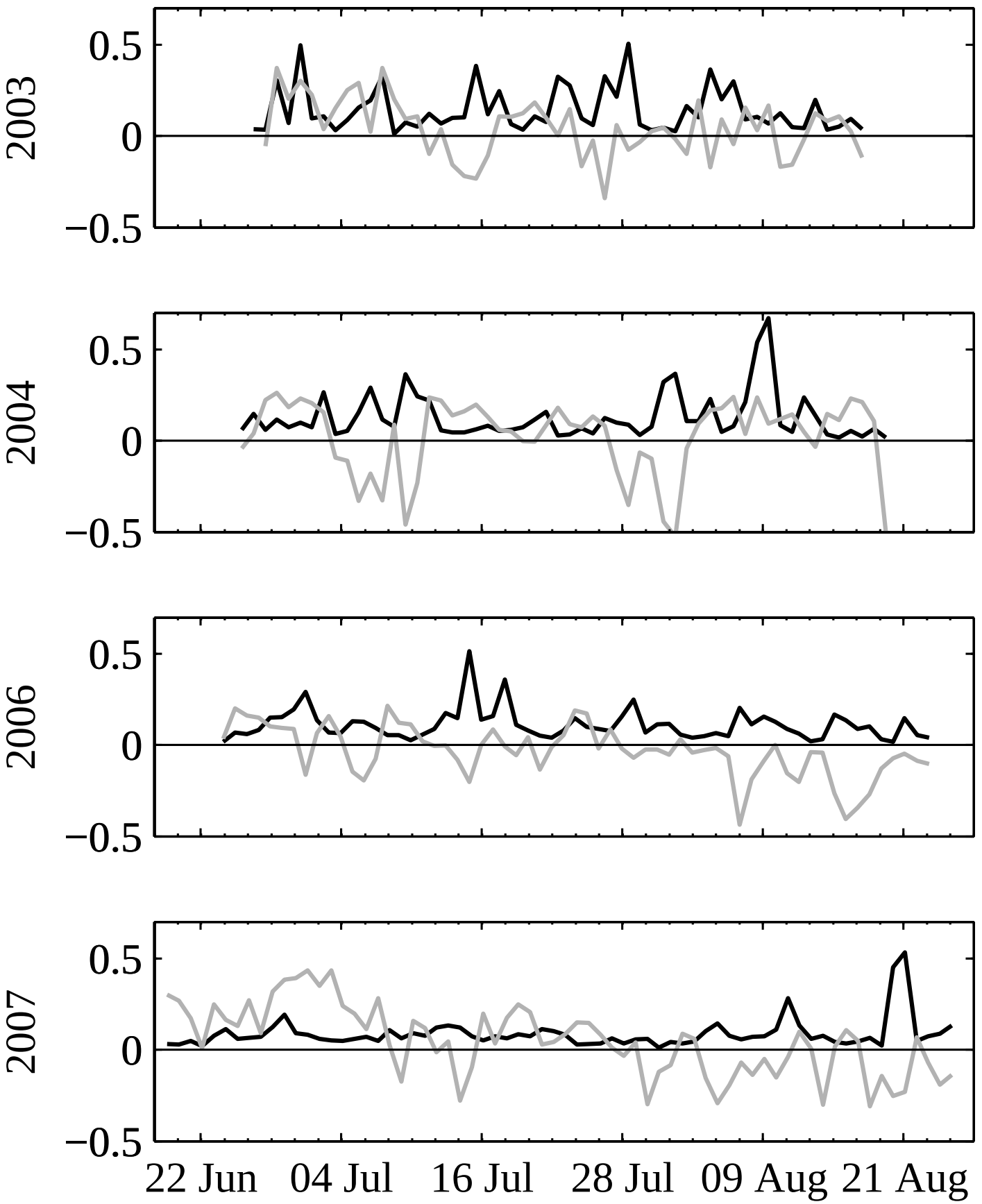
2003
2004
2006
2007
0.5
0
−0.5
22 Jun
04 Jul
16 Jul
28 Jul
09 Aug
21 Aug

Fig. 12

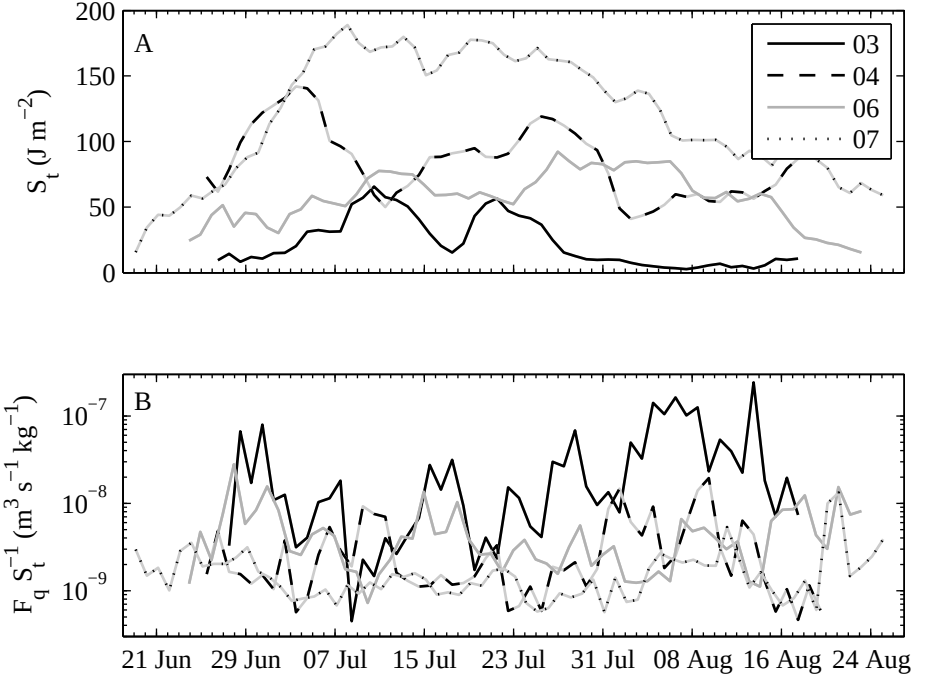
A
B
03
04
06
07
S_t (J m^{-2})
$F_q S_t^{-1}$ (m^3 s^{-1} kg^{-1})
200
150
100
50
0
10^{-7}
10^{-8}
10^{-9}
21 Jun
29 Jun
07 Jul
15 Jul
23 Jul
31 Jul
08 Aug
16 Aug
24 Aug

Fig. 13

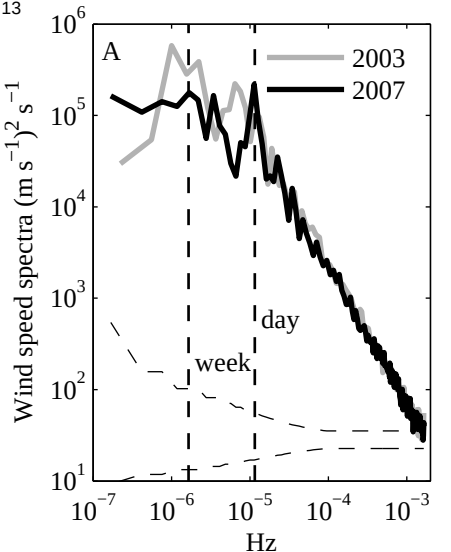
A
2003
2007
day
week
Wind speed spectra (m s^{-1})^2 s^{-1}
Hz
10^{6}
10^{5}
10^{4}
10^{3}
10^{2}
10^{1}
10^{-7}
10^{-6}
10^{-5}
10^{-4}
10^{-3}

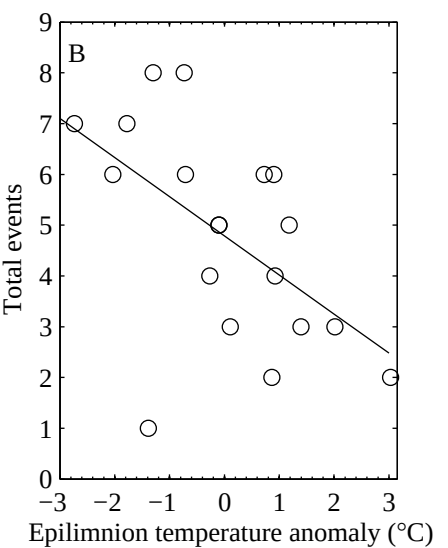
B
Total events
Epilimnion temperature anomaly (°C)
9
8
7
6
5
4
3
2
1
0
−3
−2
−1
0
1
2
3

Fig. 14

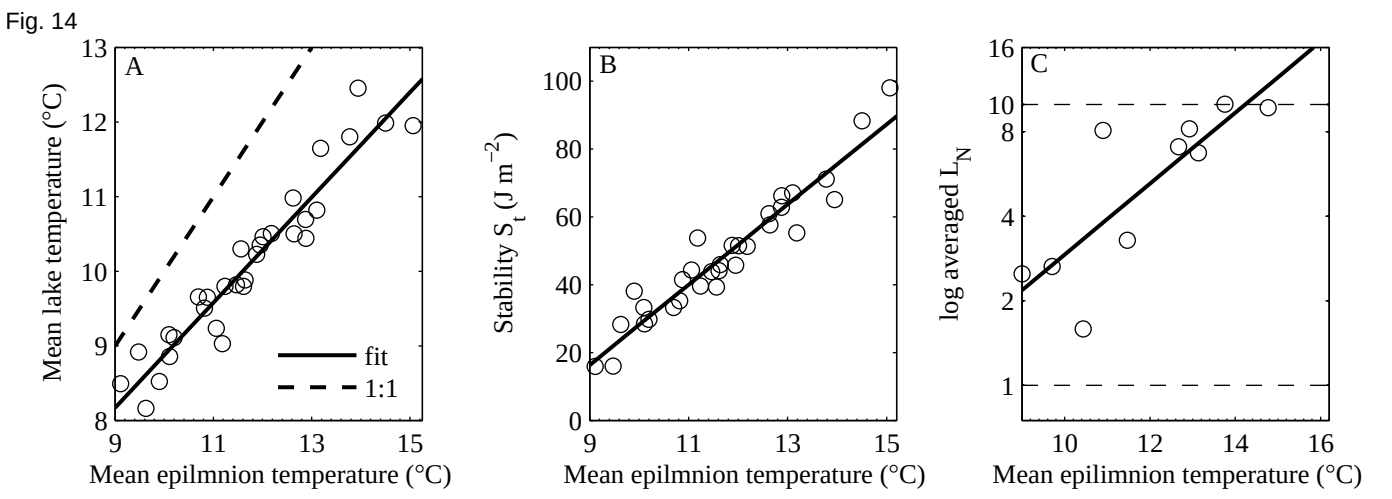
A
Mean lake temperature (°C)
Mean epilmnion temperature (°C)
fit
1:1
B
Stability S_t (J m^{-2})
Mean epilmnion temperature (°C)
C
log averaged L_N
Mean epilimnion temperature (°C)